Materials Science Forum Vol. 83-87 (1992) pp. 905-910

GENERATION OF ANION-ANTISITE DEFECTS IN n-TYPE, p-TYPE AND SEMI-INSULATING InP STUDIED BY MCD-ODMR AND MCD-ODENDOR

H.P. GISLASON[1], H. SUN[2], R.E. PEALE[2] and G.D. WATKINS[2]
[1]Science Institute, University of Iceland, Dunhaga 3, 107 Reykjavik, Iceland,
[2]Sherman Fairchild Laboratory, Lehigh University, Bethlehem PA, 18015, USA

ABSTRACT

The generation of perturbed antisite defects in n-type, p-type and semi-insulating InP by electron-irradiation with 2 MeV electrons is investigated using the sensitive optically detected electron-nuclear double resonance (ODENDOR) technique. At least two slightly different such antisite defects are distinguished by the dependence of the ODENDOR signal on irradiation dose, detection wavelength and illumination. Our results indicate that the defects are produced by the electron irradiation and are not initially present in the as-grown materials.

1. Introduction

The isolated P_{In} antisite has been observed both in as-grown and electron-irradiated p-type InP [1]. Its characteristic ODENDOR signal can be detected both via MCD in an absorption band near the band edge [1] and a photoluminescence band peaking at 0.8-0.9 eV [2]. This evidence supported by earlier ODMR results [3] agrees with the (+/++) level position of the isolated antisite being in the upper half of the bandgap, at least 0.9 eV above the valence band edge. The MCD signal was concluded to arise from photoneutralization of the P_{In}^{++} state and a subsequent excitation of the paramagnetic P_{In}^{+} state of the isolated antisite [2,4]. The isolated antisite has not been observed in as-grown n-type or semi-insulating samples and there is no unambiguous evidence that electron irradiation introduces it in such material.

Electron irradiation of n-type and semi-insulating samples as well as lightly doped p-type samples introduces an ODMR signal resembling that of the isolated antisite. The g-value and central hyperfine splitting of this signal are slightly smaller, however [2,5]. ODENDOR measurements show that this antisite defect has a distorted nearest neighbour In shell [2,4]. In this paper we show that identical antisite defects are introduced by the irradiation of n-type, p-type and semi-insulating starting material. The bulk of our evidence suggests that the perturbed antisite is not present in the as-grown samples but is produced by the e-irradiation. Also, we demonstrate that relative intensities of different peaks in the complicated ODENDOR signal depend on irradiation dose and illumination which indicates that the perturbed antisite actually comprises at least two slightly different antisite defects.

2. Experimental techniques

In an absorption measurement the transmitted intensity is $I = I_0 \exp(-\alpha d)$ where I_0 is the light intensity incident on the sample, α the linear absorption coefficient and d is the sample thickness. The dimensionless quantity $(d/4)(\alpha_+ - \alpha_-) = (I_- - I_+)/2(I_- + I_+)$ is a measure of the magnetic circular dichroism [6]. Here $I_\pm$ denotes circularly polarized light propagating towards the observer, right (+) and left (-), respectively. The diagram in figure 1 shows the paramagnetic ground state of the P_{In} antisite in InP. To the left optical transitions giving rise to MCD are schematically shown. The exact nature of the excited states is unknown, but it is not necessary to understand the optical transitions in detail in order to study the ODMR of the ground state. To the right, a splitting of the $M_S = \pm 1/2$ spin states due to central hyperfine interaction with the nuclear-spin I = 1/2 of P is illustrated. The electron spin resonance transitions $\Delta M_S = 1$, $\Delta m_I = 0$ in figure 1 are represented by the arrows labelled ODMR. The microwave absorption at resonance reduces the magnetization of the spin population and a consequent reduction of the signal as large as 30% can be observed.

The measurements were performed in an Oxford Instruments SM-4 optical cryostat with the samples mounted in a 35 GHz microwave cavity at pumped liquid He temperatures. A tungsten-iodine lamp

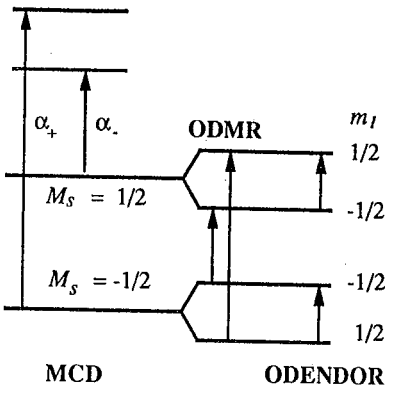

Figure 1. Paramagnetic ground state of the P_{In} antisite. Left: MCD in absorption. Right: Splitting of the $M_S = \pm 1/2$ spin states due to central hyperfine interaction with the nuclear-spin I = 1/2 of P.

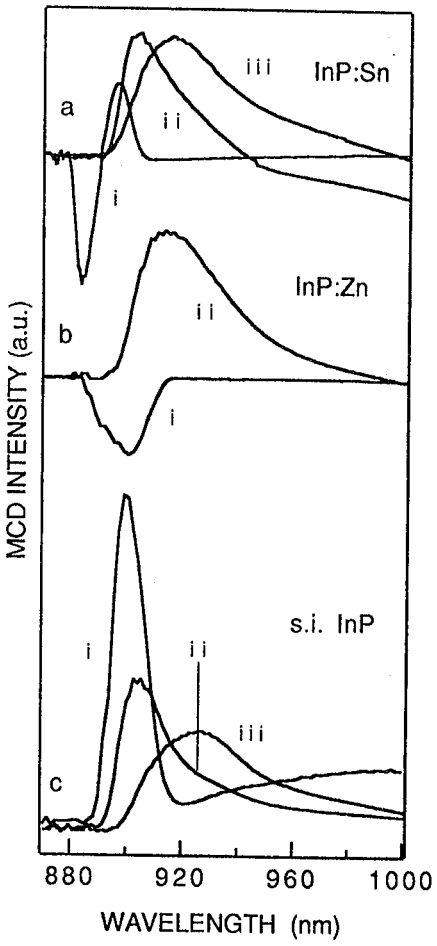

Figure 2. MCD spectra of different samples. a) n-type. b) p-type. c) Semi-insulating InP.

dispersed by a 0.25 m monochromator was used as a light source for the circularly polarized light that was generated by a linear polariser in combination with a piezoelastic modulator (Hinds PEM-3) operating at 50 kHz. The transmitted light was detected with a fast Ge detector (North Coast EO-817P) and lock-in techniques. The radio-frequency excitation for the ODENDOR experiment was generated by a frequency synthesizer (Fluke 6060B) and fed to a two-turn coil in the resonance cavity after amplification with an rf power amplifier (ENI 3100 LA).

3. MCD results

Figure 2a shows MCD spectra typical of Sn-doped InP samples ($n = 1 - 3 \times 10^{16}$ cm^{-3}) e-irradiated with 2 MeV electrons to different fluences. The signal is plotted as the difference between the MCD at 1.8 T and 0 T, thus eliminating the field-independent dichroic background. As-grown samples are characterised by a sharp negative peak close to the bandgap (curve *i*). Curve *ii* was obtained after an e-irradiation dose of 1.8×10^{17} cm^{-2} which gives rise to a positive band peaking around 900 nm. Doubling the dose ($\Phi = 3.6 \times 10^{17}$ cm^{-2}, curve *iii*) causes the MCD peak to broaden and shift to 916 nm.

As-grown Zn doped InP with $p = 5 \times 10^{15}$ cm^{-3} shows a negative MCD band at 900 nm. The MCD signal is still negative after e-irradiation to $\Phi = 1 \times 10^{16}$ cm^{-2} (figure 2b, curve *i*). Electron irradiation gradually introduces a positive band which peaks around 915 nm after an electron dose of 3×10^{17} cm^{-2} as shown in curve *ii*.

Figure 2c presents MCD spectra of a s.i. sample after different doses of e-irradiation. As-grown samples show a positive peak at 900 nm, in contrast to the n- and p-type samples in figure 2a,b. No antisite-related ODMR spectra are detected in the as-grown semi-insulating samples. Electron irradiation to $\Phi = 1 \times 10^{16}$ cm^{-2} (curve *i*), 3×10^{17} cm^{-2} (curve *ii*) and 1×10^{18} cm^{-2} (curve *iii*) reduces the intensity of the original MCD band. At the same time a paramagnetic MCD band emerges, as illustrated in figure 4c, below.

4. ODMR results

Electron irradiation of n-type, moderately doped p-type and s.i. samples generates almost identical ODMR spectra after the same irradiation dose as shown in figure 3 for $\Phi = 3 \times 10^{17}$ cm^{-2}. Curve a shows the ODMR spectrum of a Si-doped sample with $n = 5 \times 10^{15}$ cm^{-3}. Figure 3b shows the ODMR signal of a sample with $p = 5 \times 10^{15}$ cm^{-3} (compare figure 2b, curve *ii*) and the signal in figure 3c was measured in the semi-insulating sample of figure 2c, curve *ii*. All three spectra are

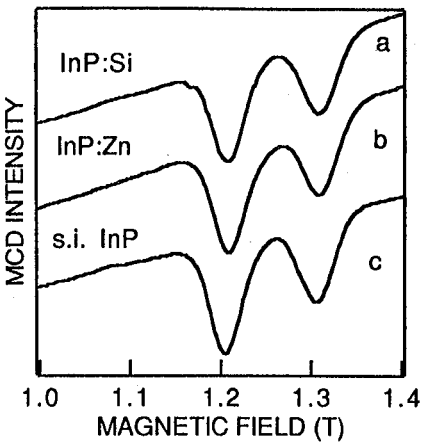

Figure 3. MCD-ODMR spectra at 910 nm.

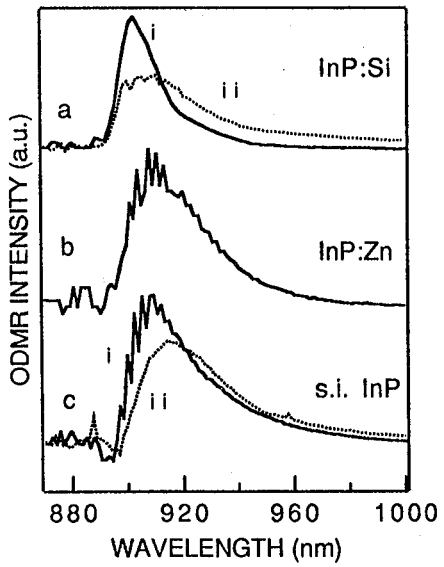

Figure 4. Spectral dependence of the ODMR signal of the samples in figure 3.

characterized by the values g = 1.990, A= (940 ± 20) x 10^{-4} cm^{-1} and half maximum width W= 410 ± 12 G which identifies them as originating from the perturbed antisite [2,4]. ODMR spectra were also measured for samples with original electron concentrations in the range 5 x 10^{15} - 2 x 10^{17} cm^{-3}, e-irradiated to the same fluence 3.6 x 10^{17} cm^{-2}. The samples show MCD spectra similar to that in figure 2, curve *iii*. ODMR signals detected at 900 nm give similar values for g, A and W as found for the spectra in figure 3.

The difference between the MCD spectra measured with the magnetic field slightly off resonance and the same spectrum measured at resonance in the low field P_{In} ODMR signal defines the spectral dependence of the P_{In} ODMR band and also the corresponding MCD band assuming a proportionality independent of wavelength. Figure 4 shows the spectral dependences of the antisite ODMR measured in the samples of figure 3. Figure 4a shows the spectral dependence measured in the InP:Si sample of figure 3a with n = 5 x 10^{15} cm^{-3}, irradiated to *i*) Φ = 3 x 10^{17} cm^{-2} and *ii*) Φ = 1 x 10^{18} cm^{-2}.

Spectral dependence measured in the same way for an InP:Zn sample with p = 5 x 10^{15} cm^{-3} irradiated to Φ = 3 x 10^{17} cm^{-2} (see figures 2b and 3b) is shown in figure 4b. Similar curves for a semi-insulating sample are shown in figure 4c, for the doses *i*) Φ = 3 x 10^{17} cm^{-2} and *ii*) Φ = 1 x 10^{18} cm^{-2}. The corresponding MCD and ODMR spectra were shown in figures 2c and 3c.

We note that the MCD-ODMR signal of the antisite is observed only for wavelengths shorter than 1000 nm in all samples. MCD signals at longer wavelengths do not contribute to the antisite ODMR. In particular, a broad band around 1200 nm is sometimes present in the spectrum, see figure 2. This MCD signal has been shown to derive from a spin-triplet defect produced by the e-irradiation. It disappears after heat treatment above 100 °C without affecting the antisite defects [7].

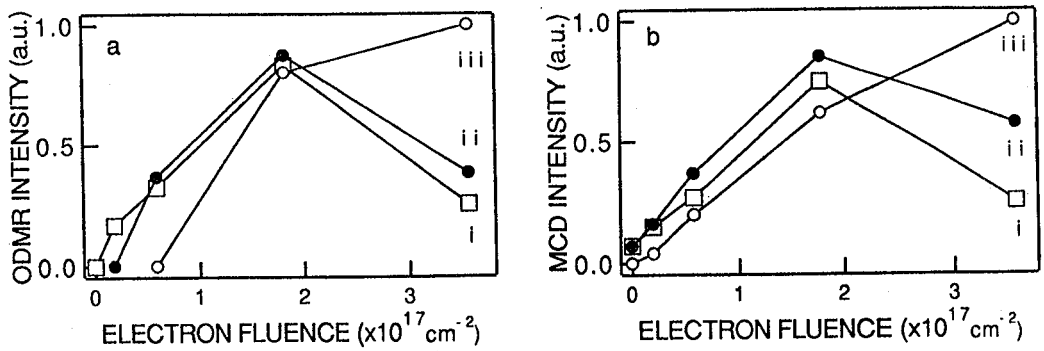

Figure 5. a) Normalized intensity of the low-field ODMR peak at 900 nm for InP:Sn samples with *i*) n = 5-9 x 10^{15}, *ii*) 1-3 x 10^{16}, *iii*) 3-20 x 10^{16} cm^{-3}. b) Normalized intensity of the corresponding MCD signals measured at 900 nm.

The intensity of the ODMR signal depends on the shallow dopant concentration and the total irradiation dose. This is illustrated in figure 5a for the InP:Sn samples, where the curves represent the magnitude of the low-field ODMR peak measured from the MCD baseline. All the spectra were measured at 900 nm. The antisite signal is not observed until the samples have been irradiated to a finite irradiation dose which increases with the shallow doping. For the n = 5-9 x 10^{15} cm^{-3} sample (curve *i*) the ODMR signal grows in linearly with dose, up to ≈ 2 x 10^{17} electrons cm^{-2}. However, for the more heavily doped materials, n = 1-3 x 10^{16} (curve *ii*) and 3-20 x 10^{16} cm^{-3} (curve *iii*), onsets are found to correspond roughly to the point of compensation of the shallow dopant by the irradiation as evidenced by the recovery in each case of the Q of the microwave cavity. The MCD band at 900 nm, on the other hand, grows in linearly without significant offset for all three samples, as shown in figure 5b, and once the ODMR signal emerges, the ODMR/MCD ratio is fairly constant. We interpret this to indicate that the perturbed antisite MCD is being produced by the irradiation and the delayed onset of the ODMR simply reflects the failure to provide sufficient microwaves in the cavity until the lossy n-type samples are compensated.

5. ODENDOR results

The ODENDOR signals of the samples in figure 3 are given in figure 6. Each spectrum was detected in the corresponding P_{In} ODMR doublet, with the field set to the low-field transition and **B** // [100]. All of the ENDOR transitions shown derive from the ^{113}In and ^{115}In nuclei of the nearest In neighbour shell of the P_{In} antisite as evidenced by the measured nuclear gyromagnetic ratio + 9.3 ± 0.5 MHz/T, which is that of the two In isotopes. All three ODENDOR signals are very similar and characteristic of the perturbed P_{In} antisite [2,4].

The In lines of ODENDOR spectrum identifying what we have referred to as the perturbed antisite are dominated by two prominent peaks at about 24 and 27 MHz as illustrated in figure 6. The angular dependence of these lines is very complex and further complicated by the fact that the In lines of the isolated antisite at 23 MHz may also be present in the spectrum, buried in the strong resonances of the perturbed In shell. The e-irradiation study indicates that the two peaks originate from slightly different defects which we refer to as $P_{In}X$ and $P_{In}Y$ for brevity. The ODENDOR spectra of figure 6 are observed after irradiation dose around 10^{17} cm^{-2}. Higher doses produce a much stronger 24 MHz peak in the n-type sample of figure 6 [2].

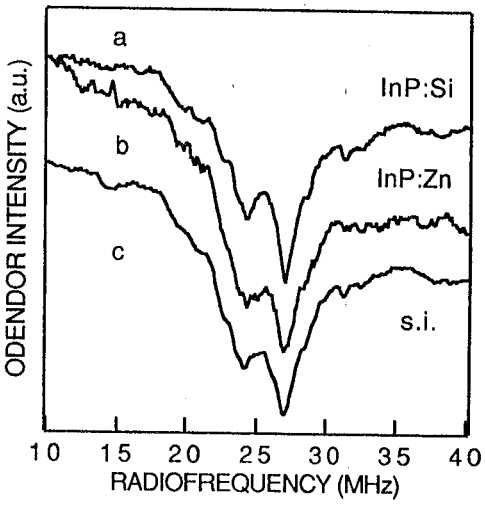

Figure 6. ODENDOR spectra of the samples in figure 3. The curves are labelled in the same way. Intensities are arbitrary.

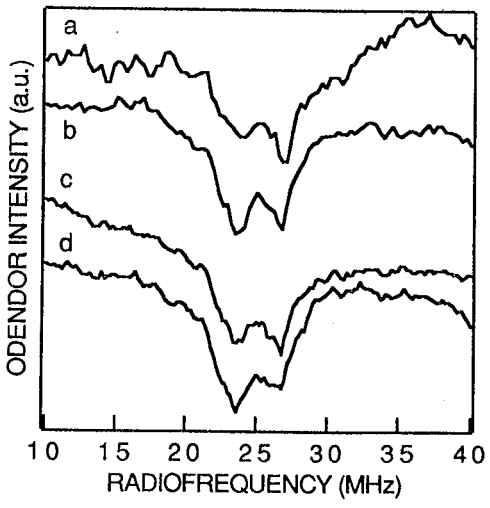

Figure 7. ODENDOR spectra of a lightly Sn-doped sample detecting the MCD either at a) 900 and b) 916 nm. Spectra detected at 916 nm: c) under illumination of white light and d) after turning the light off.

Similar but weaker effect may be observed when detecting the MCD band at different wavelengths. Figure 7 illustrates a clear tendency towards a change in the relative strength of the two ODENDOR peaks when the wavelength is changed from 900 to 916 nm in a Sn-doped sample with n = 5-9 x 10^{15} cm^{-3} irradiated to $\Phi = 3.6 \times 10^{17}$ cm^{-2}. The spectra are measured in the low-field ODMR peak detecting the MCD at 900 nm (curve a) or 916 nm (curve b). At 900 nm the 24 MHz peak is significantly weaker than the 27 MHz one, at 916 nm they are comparable in strength. The effect is much weaker for a sample with higher electron concentration (n = 1-3 x 10^{16} cm^{-3}) and not detectable for a sample with n = 3-20 x 10^{16} cm^{-3}. Similar effect is observed in more lightly irradiated samples, except that the 24 MHz peak is even weaker than that in figure 7.

If the sample in figure 7b is illuminated with white light a weak but reproducible shift in the relative intensity of the 24 and 27 MHz ODENDOR peaks is observed as figure 7c and d demonstrate. Spectrum c was taken under identical conditions as spectrum b, except that the sample was continuously illuminated with white light from a Xe arc source. Evidently, the relative strengths of the 24 and 27 MHz lines have changed. When the white light is turned off, the spectrum recovers as shown in curve d. Figure 7 indicates that the defect, which we have referred to as the perturbed antisite, actually comprises at least two slightly different defects or defect configurations. These will be referred to as $P_{In}X$ and $P_{In}Y$, respectively, the X and Y denoting impurity atoms or other distortion in the nearest neighbour In shell.

6. Discussion

The paramagnetic P_{In}^{+} state of the isolated antisite is long-lived enough that two-step excitation via the state can take place [2,4]. This allows MCD-detection of P_{In}^{+} in as-grown lightly doped p-type material, although the (+/++) level is almost 1 eV above the valence band edge. In most as-grown p-type samples no antisite signals are observed, however, presumably because the acceptors provide fast recombination channels. Electron irradiation passivates these channels and P_{In}^{+} can be observed either directly, if the charge state is right, or via two-step excitation.

The perturbed antisite of the present work has been observed in widely different samples, n-type, p-type and semi-insulating after e-irradiation, but never in as-grown material. The irradiation therefore either produces the perturbed antisite or reveals its paramagnetic state. If the perturbed antisite is a neutral $(P_{In}^{+}\text{-}A_{In}^{-})^{o}$ pair it is very likely to be a fast recombination centre in contrast to the isolated P_{In}. Optical excitation is unlikely to build up high enough population for two-step excitation of its paramagnetic state. It can therefore be argued that the defect has to be in the paramagnetic state to begin with if it is to be detected in MCD and could be present in as-grown p-type and s.i. samples, albeit undetected. In view of the energy position of the P_{In}^{+} state of the isolated antisite, at least 0.9 eV above the valence band, the less electronegative $(P_{In}^{+}\text{-}A_{In}^{-})^{o}$ state of the perturbed one is likely to be even higher in the bandgap [4]. Hence, the paramagnetic $(P_{In}^{+}\text{-}A_{In}^{-})^{o}$ state may escape detection in p-type and semi-insulating material, where the Fermi level would always be too low.

For p-type samples the e-irradiation completely compensates the shallow acceptors and converts the samples to n-type [8]. The sample of figure 2b with p = 5 x 10^{15} cm^{-3} shows a weak ODMR signal after an irradiation dose of $\Phi = 1 \times 10^{16}$ cm^{-2}. This dose also makes the sample high-ohmic n-type [8]. For p-type samples with higher hole concentrations larger irradiation doses are needed in order to detect the antisite ODMR. If the perturbed antisite existed undetected in as-grown p-type samples the e-irradiation could be revealing its paramagnetic state simply by converting the sample to n-type.

In the semi-insulating samples, there are no shallow carriers to be compensated. Yet, there is no detectable ODMR signal for irradiation doses below 10^{16} cm^{-2}. Further irradiation generates the antisite signal in a similar way as found in the n- and p-type samples and shown in figure 4. Saturation occurs in a similar range, $\approx 5 \times 10^{17}$ cm^{-2}. The originally semi-insulating samples turn n-type upon e-irradiation as determined by our Hall measurements, and once again the emergence of the perturbed antisite could be explained by the shift of the Fermi level.

The study in the n-type samples, however, provides strong evidence that the perturbed antisite is not present in the as-grown state of these materials but is being produced by the irradiation. The

arguments are as follows: (1) The constant ODMR/MCD ratio versus electron flux once the n-type samples are sufficiently compensated identifies the 900 nm MCD band with the paramagnetic charge state of the perturbed antisite. (2) The 900 nm MCD band is absent in the as-grown n-type samples and grows in linearly vs. irradiation flux until it saturates at $\approx 2 \times 10^{17}$ e/cm^{-2}. (3) The linear growth reveals that the defect is in the correct paramagnetic charge state at the outset in the n-type material and therefore is a direct measure of the perturbed antisite concentration. [This is consistent with the $(P_{In}^{+}\text{-}A_{In}^{-})^{o}$ model which would not be expected to have an additional acceptor (-/o) state in the gap].

An unexpected result is the apparent saturation in all materials at approximately the same MCD intensity. This might have been interpreted more easily as evidence that the defects were already present and simply being revealed by the Fermi level effect. Indeed this was our original tentative conclusion that promted the detailed studies we report here in the n-type material. We are forced, however, to conclude from these n-type studies that the weight of the evidence strongly indicates that the perturbed antisite is being produced by the irradiation.

In conclusion, the generation by e-irradiation of the perturbed antisite as monitored by MCD-ODMR and MCD-ENDOR in p-type and s.i. InP could be explained simply by the conversion to n-type, revealing defects already present. However, detailed studies in n-type material provide strong evidence that the defects are not present initially but are actually being produced by the irradiation. In addition, we find that minor differences in the relative intensities of the In lines of the ODENDOR spectrum suggest that more than one slightly different configurations of the perturbed antisite exist.

7. Acknowledgements

The research was supported by National Science Foundation Grant No. DMR-85-20269, NATO Scientific Affairs Division Grant No. 0499/87 and the Icelandic Council of Science.

REFERENCES

1. D.Y. Jeon, H.P. Gislason, J.F. Donegan, and G.D. Watkins, Phys. Rev. B**36**, 1324 (1987)
2. H.P. Gislason, H. Sun, F. Rong, and G.D. Watkins, in *The Physics of Semiconductors*, Vol. 3, ed. E.M. Anastassakis and J.D. Joannopoulos (World Scientific, Singapore 1990) p. 666
3. L.H. Robins, P.C. Taylor, and T.N. Kennedy, Phys. Rev. B**38**, 13227, (1988)
4. H.P. Gislason, F. Rong, H. Sun and G.D. Watkins, to be published.
5. A. Kana´ah, M. Deiri, B.C. Cavenett , T.A. Kennedy, and N.D. Wilsey, J. Phys. C**18**, L619 (1984)
6. See e.g. N.V. Starostin and P.P. Feofilov, Soviet Physics Uspekhi **12**, 252 (1969)
7. H.P. Gislason, D.Y. Jeon, G.D. Watkins and K. Ando, Materials Science Forum **38-41**, 1145 (1989)
8. K. Ando, A. Katsui, D.Y. Jeon, G.D. Watkins and H.P. Gislason, Materials Science Forum **38-41**, 761 (1989)